Bachelor's Thesis

High-order harmonic generation using variably polarized two-color fields

Author:
Hampus Wikmark

Supervisor:
Christoph Heyl

September 2, 2013

Contents

1 Introduction

A field of study that has gained prominence in the last twenty years is *high order harmonic generation*, a subset of nonlinear optics, both of which will be described here. With the help of an intense laser field and a generating medium, extremely short wavelength light can be produced.

Since the generation of harmonics is due to the interaction between the laser field and atomic electrons in the medium, the harmonics generated can give a wealth of information about the electronic structure of the atoms and molecules, which makes it a very interesting tool in atomic physics.

Applications in other fields are easily envisioned when one considers that the harmonics generated are in the extreme ultraviolet and X-ray spectra. Radiation in this energy region is already produced in synchrotron storage rings for the benefit of sciences such as biology, chemistry and materials sciences.

This thesis considers higher-order harmonic generation (HHG) by a *two-color* laser field, in which two fields, one with a frequency twice that of the other, is used. There are two main reasons for doing this; it affords greater control of the generating process, and it enables measurement of the ionization time.

The effects on generation can then be studied as functions of the difference both in phase and in polarization between the two fields.

HHG with two-color laser fields is not a new subject, and there have been several experiments performed, in several different configurations, most of which, however, have only considered either the case when the fields have fully parallel or fully perpendicular linear polarizations with regards to each other. Here, cases "in between" these extremes are considered, in trying to establish a model for arbitrarily polarized two-color fields.

The work consists of theoretical work and simulations, based on the models already proposed in this field, as well as analysis of experimental data previously collected at the atomic physics department of Lund University. Models for harmonic generation in both parallel and perpendicular configurations are tested, and the aim is to unite them and reconcile them with the data.

It turns out that most of the models seem to give good explanations and predictions, and that assumptions given in this report generally prove accurate.

Glossary

This paper contains a number of acronyms and terms, most explained in context but also given here for convenience:

- **Laser -** Light Amplification by Stimulated Emission of Radiation is a technique exploiting various electronic properties of materials to enable the production of extremely coherent and/or intense light.
- **Harmonic -** A harmonic of an electromagnetic wave is the same as a harmonic of a sound wave, an integer multiple of its frequency.
- **HHG -** High-order Harmonic Generation is the process by which an intense field of (comparatively) low photon energy laser radiation interacts with atoms, creating highly energetic photons.
- **Two-color fields -** A two-color laser field is a field that consists of laser radiation of two different wavelengths (colors), in this case a $\omega-2\omega$ field, i.e. a laser beam combined with its second harmonic (twice the frequency of the fundamental beam).
- **KDP -** Potassium dihydrogen phosphate is a crystal with a variety of interesting optical properties, notably being suitable for second harmonic generation.
- **ADK model -** The ADK (Ammosov, Delone, Krainov) model describes atomic ionization in very strong electromagnetic fields (see equation (4) on page 7) [1].
- **Differentiation -** This thesis mostly uses the time differentiation convention $\dot{x} = \frac{dx}{dt}$ and $\ddot{x} = \frac{d^2x}{dt^2}$.

2 Theory

2.1 Electromagnetic radiation

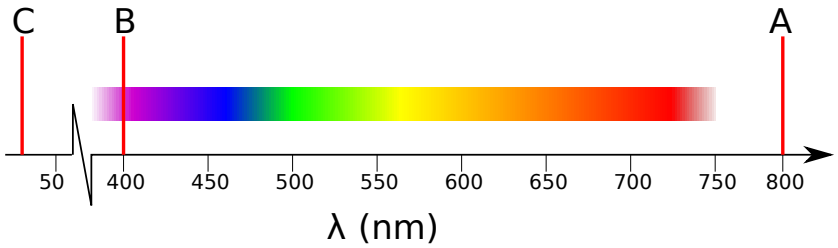

Figure 1: The electromagnetic spectrum, along with a few points of interest: **A**, the fundamental field, **B**, the second harmonic (**A** and **B** making up the two-color field), and **C**, the 25th harmonic, which is one of the harmonics measured in the experiment.

This report concerns electromagnetic radiation with different central wavelengths and thus photon energies. The fundamental beam of the laser has a wavelength of 800 nm which puts it in the Near IR range, and has a photon energy of around 1.55 eV. Its second harmonic has a wavelength of 400 nm, which corresponds to (visible) violet light, and twice the energy (3.1 eV). However, they are colloquially referred to as the ”red” and ”blue” beam, respectively.

The high harmonics reached are in the XUV (eXtreme Ultraviolet) or even soft X-ray ranges, with photon energies of around 40-60 eV (wavelengths down to around 20 nm).

In many cases, one is interested in the frequency, ν, of the radiation, but for reasons that will become apparent, most calculations in this paper instead use the angular frequency, $\omega = 2\pi\nu$. For this reason the red and blue fields are also referred to as the ω and 2ω fields.

2.2 Strong fields

The following theory deals mainly with the so-called *strong fields* regime, that is, highly intense laser fields. There is no clear boundary to strong fields, but normally fields with intensities on the order of 10^{14} W/cm^2 and above are considered strong. This is the scale on which they become comparable to the atom's Coulomb potential.

To achieve these very high intensities, highly focused and very short (tens of femtoseconds and shorter) laser pulses are used. More on this can be found in section 3.1 on page 21.

2.3 Nonlinear optics

Nonlinear optics deals with optical media that have a nonlinear relation between the polarization density and the electric field [8, p. 877]. In the "normal" case, this relationship is simply linear,

$$\mathcal{P} = \epsilon_0 \chi E, \tag{1}$$

where ϵ_0 is the permittivity of the vacuum and χ is the electric susceptibility of the medium. In the presence of strong fields (see the previous section), however, this response may become nonlinear, and can better be described as a Taylor series:

$$\mathcal{P} = a_1 E + \frac{1}{2} a_2 E^2 + \frac{1}{6} a_3 E^3 + \ldots, \tag{2}$$

where a_1, a_2 and a_3 are the first, second and third derivatives of $\mathcal{P}$ with regards to E, a_1 then corresponding to the linear relation $\epsilon_0 \chi$. This makes it obvious that the prominence of the later terms increases with the field strength. Normally this is written as

$$\mathcal{P} = \epsilon_0 \chi E + 2d\chi^{(2)} E^2 + 4\chi^{(3)} E^3 + \ldots, \tag{3}$$

where $d = \frac{1}{4} a_2$ and $\chi = \frac{1}{24} a_3$. These describe the second (depending on $\chi^{(2)}$) - and third (depending on $\chi^{(3)}$) order effects. The total polarization density can then be described as $\mathcal{P} = \epsilon_0 E + \mathcal{P}_{\mathrm{NL}}$, where $\mathcal{P}_{\mathrm{NL}}$ comprises all the terms in equation (3) apart from the first one, i.e. all the nonlinear parts.

Some crystalline materials exhibit a very strong d component, and thus provide efficient second-harmonic generation. One of these is KDP, or potassium dihydrogen phosphate.

Materials that, in contrast with crystals, are isotropic (they are not "arranged" along any particular dimension), do not exhibit this second-order effect, because this requires a different response to E and $-E$ (otherwise the $\mathcal{P}$ response would not be the same). However, it is perfectly possible for them to have a strong $\chi^{(3)}$ component, and generate third, and subsequent odd, harmonics.

High-order harmonics are not quite described by this theory, as it depends on additional factors such as ionization. However, the isotropicity of gases means that, using only one field, HHG will only result in odd harmonics.

2.4 The three-step model

The so-called *simple man's model* or three-step model is a semi-classical model, featuring a series of assumptions about the manner in which strong fields interact with atomic electrons [4]. Taken broadly, it assumes that higher harmonic generation occurs in three steps:

- **Tunneling Ionization:** The strong laser field distorts the atomic potential, lowering the potential barrier to a level where the electron may tunnel out of the atom's potential and enter the continuum outside. As tunneling is a quantum phenomenon, this must obviously be given a "quantum treatment".

- **Propagation:** When the electron has left the potential of the atom, it is acted upon by the field of the laser. This causes it to move around and, in certain cases, move back towards the atom, having gained kinetic energy by acceleration in the electromagnetic field. Just dealing with electrons in electromagnetic fields, it (generally) suffices to calculate this classically.

- **Recombination:** If and when the electron comes back to the atom, it may recombine, that is, assume its place in the atom. When this happens, a photon is emitted, the energy of which is equal to the sum of the atom's potential and the kinetic energy acquired by the electron. This is also, as implied by the wave-particle duality assumed, a quantum phenomenon.

Ionization

In atoms, as can be seen in figure 2a on the next page, the elctron is constrained by its Coulomb attraction to the nucleus into what's called a *potential well*. This well presents a "barrier" that the electron doesn't have sufficient energy to overcome.

A strong laser field presents an electro-magnetic (EM) field, which affects all charged particles, including the electrons in the atom. If the field strength

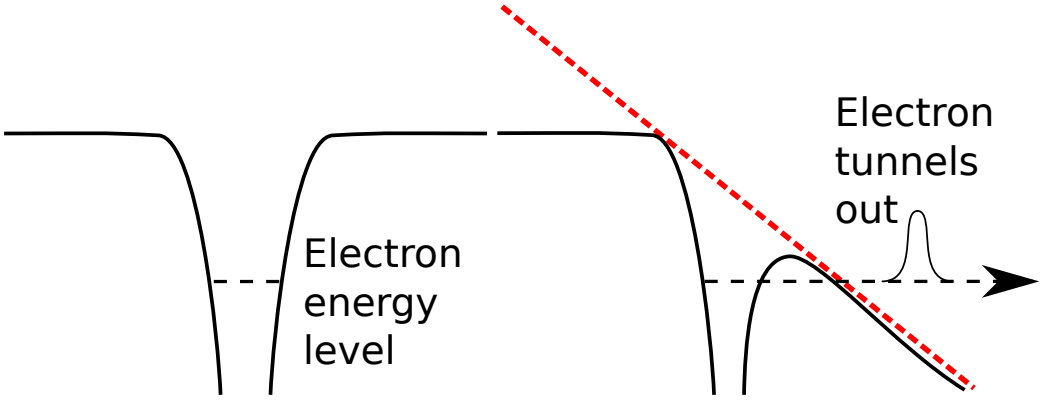

(a) Atomic potential. **(b)** Atomic potential affected by a strong field.

Figure 2: An illustration of tunneling ionization: **(a)** shows the normal atomic potential, and **(b)** shows how this potential is deformed by the strong laser field.

is sufficiently great it will, in essence, deform the atomic potential. An illustration of this can be seen in figure 2b. The electron may then, in certain cases, be able to tunnel out through this potential barrier.

Since the EM field of the laser is fluctuating (normally assumed as a simple sine or cosine function), the ionization probability also varies. However, if the wavelength of the laser is much greater than the size of the atom[1], the ionization rate Γ across the atom at any given moment can be assumed to be homogenous and dependent on the amplitude of the field (according to the so-called ADK model [1]) as

$$\Gamma(t) = 4\omega_0 \left(\frac{I_p}{E_h}\right)^{5/2} \frac{E_a}{E(t)} \exp\left[-\frac{2}{3}\left(\frac{I_p}{E_h}\right)^{3/2} \frac{E_a}{E(t)}\right], \tag{4}$$

where ω_0 is the atomic frequency unit ($4.13{\cdot}10^{16}$ s^{-1}), E_h is the ionization potential of hydrogen (13.6 eV), I_p is the ionization potential of the element used (in this case, argon, 15.6 eV), E_a is the atomic unit of the electric field ($5.14{\cdot}10^{11}$ V/m), and $E(t)$ is the electric field at the given time t, which is related to the field intensity I as

$$I(t) = \frac{1}{2}\epsilon_0 c|E(t)|^2, \tag{5}$$

where ϵ_0 is the permittivity the vacuum and c is the speed of light in vacuum. This model also needs a series of quantum mechanical corrections described by [3].

[1]Compare, to take an example from this experiment, the 800 nm laser wavelength and the atomic radius of argon (on the order of 0.07 nm [2]).

Propagation

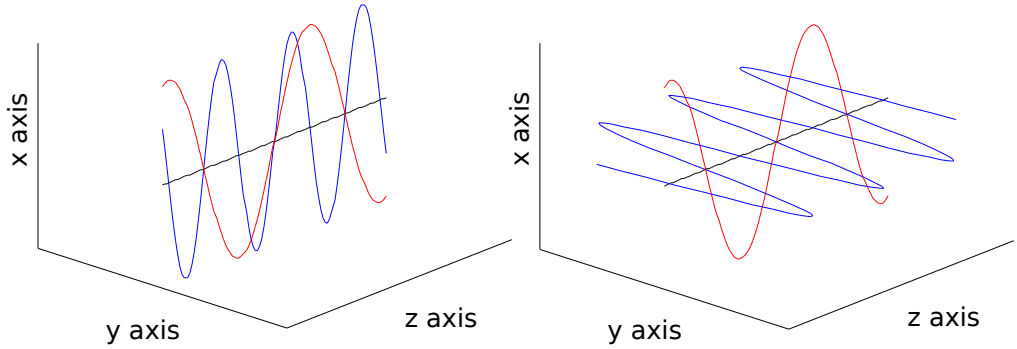

(a) The ω and 2ω fields being parallel. **(b)** The ω and 2ω fields as perpendicular.

Figure 3: The two extreme modes of polarization: **(a)** shows the two fields as parallel and **(b)** shows them as perpendicular. Note, however, that in the actual experiment the "blue" field was much weaker.

When the electron has exited the atom through tunnel ionization, it can be assumed to move classically in the EM field produced by the laser.

The first case, which can be seen in figure 3a, is when the ω and 2ω fields are both completely linearly polarized along the x axis. Assuming that the field at time t is given by

$$E_x(t) = E_0 \left(\cos(\omega t) + \alpha \cos(2\omega t + \phi)\right), \tag{6}$$

where E_0 is the field's maximum strength, α is the relative amplitude of the 2ω field with respect to the ω field, and ϕ is the phase difference, the force upon the electron is

$$F_x(t) = eE_x(t) = eE_0 \left(\cos(\omega t) + \alpha \cos(2\omega t + \phi)\right). \tag{7}$$

The electron is assumed to just appear outside the potential at a given time t_i. The acceleration is then described as

$$\ddot{x}(t) = \frac{F(t)}{m} = \frac{eE_0}{m} \left(\cos(\omega t) + \alpha \cos(2\omega t + \phi)\right), \tag{8}$$

where m is the electron mass and e the electron charge. The velocity is then

$$\dot{x}(t) = \int_{t_i}^{t} \ddot{x}\ dt' = \int_{t_i}^{t} \frac{eE_0}{m} \left(\cos(\omega t') + \alpha \cos(2\omega t' + \phi)\right) dt' =$$
$$= \frac{E_0 e}{m\omega} \left(\sin(\omega t_i) - \sin(\omega t) + \frac{\alpha}{2} \left(\sin(2\omega t_i + \phi) - \sin(2\omega t + \phi)\right)\right), \quad (9)$$

where t_i represent the ionization time, that is, the time at which the electron exits the atom. To know the velocity of the atom at the return time t_r, it is inserted as t so the velocity becomes

$$\dot{x}(t_r) = \frac{E_0 e}{m\omega} \left(\sin(\omega t_i) - \sin(\omega t_r) + \frac{\alpha}{2} \left(\sin(2\omega t_i + \phi) - \sin(2\omega t_r + \phi)\right)\right). \quad (10)$$

Likewise, from the velocity of the electron, its position at the time t can be calculated:

$$x(t) = \int_{t_i}^{t} \dot{x}\ dt' = \int_{t_i}^{t} \frac{E_0 e}{m\omega} \left(\sin(\omega t_i) - \sin(\omega t') + \frac{\alpha}{2} \left(\sin(2\omega t_i + \phi) - \sin(2\omega t' + \phi)\right)\right) dt' =$$
$$= -\frac{eE_0}{4m\omega^2} (\omega(4(t_i - t)\sin(\omega t_i) + 2\alpha(t_i - t)\sin(2\omega t_i + \phi))$$
$$+ 4(\cos(\omega t_i) - \cos(\omega t)) + \alpha(\cos(2\omega t_i + \phi) - \cos(2\omega t + \phi))), \quad (11)$$

which at $t = t_r$ becomes

$$x(t_r) = -\frac{eE_0}{4m\omega^2} (\omega(4(t_i - t_r)\sin(\omega t_i) + 2\alpha(t_i - t_r)\sin(2\omega t_i + \phi))$$
$$+ 4(\cos(\omega t_i) - \cos(\omega t_r)) + \alpha(\cos(2\omega t_i + \phi) - \cos(2\omega t_r + \phi))). \quad (12)$$

Another basic case, seen in figure 3b on the preceding page, is when the ω and 2ω field are perpendicularly polarized with regards to each other. For simplicity's sake it is assumed that the ω field is polarized along the x axis and the 2ω field along the y axis, with direction of propagation along the z axis.

For the velocity and position in the x direction, equation (10) and equation (12) can be used, with α simply being zero (the second harmonic field has no component in the x direction).

For the y direction, the electron is affected the same way by the 2ω field as in the previous example (F_y having the same expression as F_x but with

another field). This means that one may use only the terms in equations (10) and (12) which are multiples of α. This leads to the following expressions:

$$\begin{aligned}\dot{y}(t) = \int_{t_i}^{t} \ddot{y}\ dt' = \int_{t_i}^{t} \frac{eE_0}{m} \left(\alpha \cos(2\omega t' + \phi)\right) dt' = \\ = \frac{E_0 e}{m\omega} \left(\frac{\alpha}{2} \left(\sin(2\omega t_i + \phi) - \sin(2\omega t + \phi) \right) \right), \end{aligned} \tag{13}$$

which at t_r is

$$\dot{y}(t_r) = \frac{E_0 e}{m\omega} \left(\frac{\alpha}{2} \left(\sin(2\omega t_i + \phi) - \sin(2\omega t_r + \phi) \right) \right), \tag{14}$$

and

$$\begin{aligned} y(t) = \int_{t_i}^{t} \dot{y}\ dt' = \int_{t_i}^{t} \frac{E_0 e}{m\omega} \left(\frac{\alpha}{2} \left(\sin(2\omega t_i + \phi) - \sin(2\omega t' + \phi) \right) \right) dt' = \\ = -\frac{eE_0}{4m\omega^2} (\omega(2\alpha(t_i - t) \sin(2\omega t_i + \phi)) \\ + \alpha(\cos(2\omega t_i + \phi) - \cos(2\omega t + \phi))), \end{aligned} \tag{15}$$

which finally comes out to

$$\begin{aligned} y(t_r) = -\frac{eE_0}{4m\omega^2} (\omega(2\alpha(t_i - t_r) \sin(2\omega t_i + \phi)) \\ + \alpha(\cos(2\omega t_i + \phi) - \cos(2\omega t_r + \phi))), \end{aligned} \tag{16}$$

Knowing these two cases, the general model for propagation can be constructed, assuming the x and y components of the electric field are independent.

To calculate any given aspect of propagation (acceleration, velocity, or position), one simply has to take the two equations, for the x and y component, then replace α with $\alpha \cos(\Theta)$ in the x equation, and $\alpha \sin(\Theta)$ in the y equation, where Θ is the angle between the polarization of the ω and 2ω fields.

Recombination

When the electron returns to the atom, it has gained additional kinetic energy from the field. This kinetic energy (the *return energy*) depends on when it was released and when it returns, as well as the ionization potential of the atom itself. When it recombines, this 'excess' energy leads to a photon being emitted. The maximum energy the electron can receive (when I_p, the ionization potential, is greater than U_p) [6] is

$$E_e = I_p + 3.17\ U_p \tag{17}$$

where U_p is the so-called *ponderomotive energy*. It represents the average energy given by the field to the electron, and can be calculated as

$$U_p = \frac{e^2 E_0^2}{4m\omega^2}. \tag{18}$$

The return energy, and return time, dependence on the ionization time t_i can be calculated numerically, by using the propagation equations starting on page 8, and keeping track of when the electron returns to $x = 0$. This is seen in figure 4 on the next page. The red marker in the figure separates the *long* and *short* trajectories, which describe the time in duration of the electron's journey (and, by extension, the ionization time). For phase matching reasons (see section 2.9 on page 20), the short trajectories are most commonly observed.

The kinetic energy can be written classically as $mv^2/2$, which can be confirmed by examining the expression for the velocity $\dot{x}$ in equation (10) on page 9.

The frequency and wavelength of the photon can then be calculated using Planck's familiar

$$E_\gamma = h\nu = \frac{hc}{\lambda}. \tag{19}$$

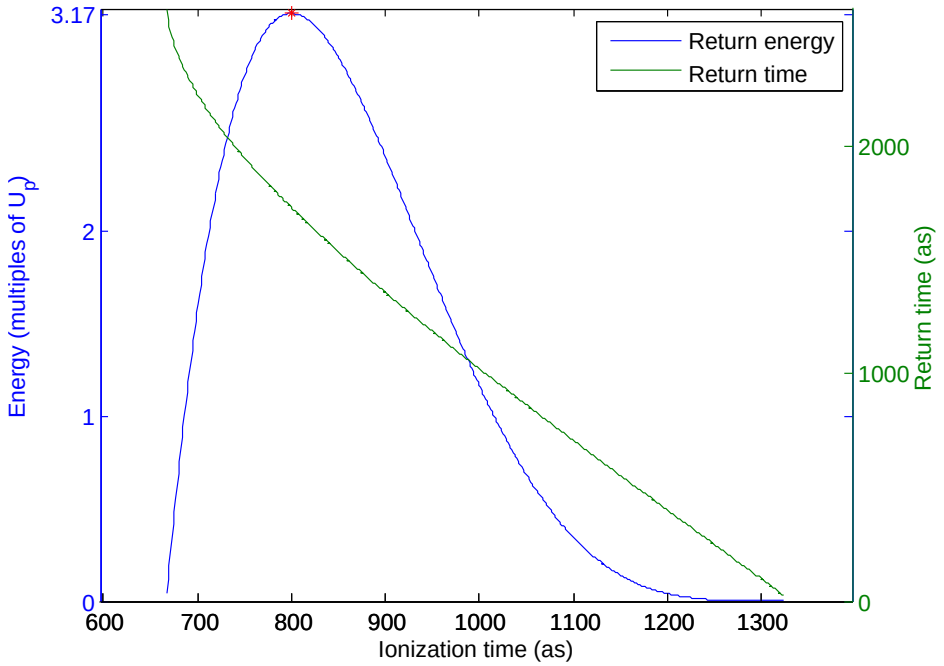

Figure 4: The return energy and return time of the electron, as a function of ionization time. The only field used here is the ω field, and $t = 0$ is the starting point of its sinoid shape. Note the red marker separating the long (to the left) and short (to the right) trajectories. These are so named because the long trajectories leave the atom earlier and thus have a longer journey.

2.5 Harmonic spectrum

The ionization in this experiment takes place in a gas, which is isotropic (i.e. shows no significant changes in relevant characteristics over any particular direction). This means that the ionization rate when the field is E is the same as when it's $-E$, and gives a $T/2$ periodicity (T being the laser period)[2].

This periodicity of $T/2$ in the time domain leads to a periodicity of 2ω in the frequency domain, i.e., when recombination occurs (see section 2.4 on the previous page) photons of every other harmonic (multiple of the fundamental frequency) are emitted. Since the first (fundamental) frequency is there, subsequent harmonics will be odd.

[2]See section 2.2 on page 4 for a brief explanation of this.

To achieve even harmonics as well, one may perturb the field in a way that the two π periods are no longer identical, thus leading to T periodicity in the time domain and ω in the frequency domain. One way of doing so[3] is to have a weak second harmonic beam copropagating with the fundamental beam. The total generating field can then be described as in equation (6) on page 8.

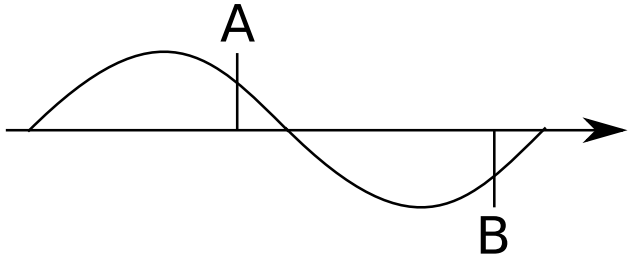

Figure 5: An illustration of two points at the same time in each half cycle.

The amplitudes of the even harmonics, then, depend on the level of difference between these two half cycles. Given two points separated by half a (fundamental) cycle (see figure 5), they can be approximated to be Dirac delta functions. The amplitude 'function' at the given points then reads as [4]

$$f(t) = \sum_n A\delta(t - nT) - B\delta(t - nT + \frac{T}{2}), \tag{20}$$

where A, B is their amplitude and T is the period of the fundamental (IR) field. In the frequency space, this function corresponds to the Fourier transform:

$$\mathcal{F}(\omega) = \frac{A}{T}\sum_n \delta(\omega - n\Omega) - \frac{B}{T}\sum_n \delta(\omega - n\Omega)\exp\left(-i\frac{T\omega}{2}\right), \tag{21}$$

where $\Omega = 2\pi/T$.

If $n = 1,\ 3,\ 5...$ (odd harmonics), the expression simplifies to

$$\mathcal{F}(n\Omega) = \frac{A}{T} - \frac{B}{T}\exp(-ni\pi) = \frac{A}{T} + \frac{B}{T}, \tag{22}$$

[3]The way this is done in the experimental part.

and the amplitude of the odd harmonics is thus proportional to $A + B$.

If $n = 2,\ 4,\ 6...$ (even harmonics), it instead gives the exponential

$$\mathcal{F}(n\Omega) = \frac{A}{T} - \frac{B}{T}\exp(-ni\pi) = \frac{A}{T} - \frac{B}{T}, \tag{23}$$

making the even harmonics proportional to $A - B$.

Complicating this further is the fact that differences in the electric field between the half cycles can also lead to a phase difference between harmonics emitted from the two. The phase of the emitted harmonic field [7] can be calculated as

$$\Sigma = -\frac{S(p, t_i, t_r)}{\hbar} + q\omega t_r \tag{24}$$

where q is the harmonic order, ω is the angular frequency of the laser field, t_i and t_r are the ionization and recombination times, respectively, and $S(p, t_i, t_r)$ is the *quasiclassical action*, calculated as

$$S(p, t_i, t_r) = \int_{t_i}^{t_r} dt \left(\frac{p^2(t)}{2m_e} + I_p\right) \tag{25}$$

where $p(t)$ is the momentum of the electron at the time t, m_e is the electron mass (making the first term the kinetic energy of the electron), and I_p is the ionization potential. Assumptions have previously been made that this difference in phase proves a greater impact on the harmonic spectrum than the amplitude difference [4].

Considering this phase shift, equation (20) on the preceding page can be rewritten as

$$f(t) = \sum_n A\delta(t - nT)e^{i\Sigma_1} - B\delta(t - nT + \frac{T}{2})e^{i\Sigma_2}, \tag{26}$$

where Σ_1 and Σ_2 are the phases given by equation (24), or

$$f(t) = \sum_n A\delta(t - nT) - B\delta(t - nT + \frac{T}{2})e^{i\Sigma_3}, \tag{27}$$

where $\Sigma_3 = \Sigma_2 - \Sigma_1$.

After this is done, multiplying by the constant T modifies equations (22) and (23) to

$$\mathcal{F}(n\Omega) = \begin{cases} A + B\exp(-i\Sigma_3), & n \text{ odd} \\ A - B\exp(-i\Sigma_3), & n \text{ even.} \end{cases} \tag{28}$$

2.6 Ionization gate

Equation (4) on page 7 and its modifications, along with the phase and amplitude modifications in the previous chapter, make up the so-called *ionization gate*[4]. This is one of the modulation models assumed to govern the harmonic spectrum, especially when the ω and 2ω fields are polarized in parallel with each other.

The energy can be calculated as a function of the ionization time (see figure 4 on page 12), and the ionization time can thus be inferred from the energy. Knowing the energy of a harmonic order,

$$E_q = qh\nu, \tag{29}$$

where q is the harmonic order, the field strength can be calculated at the ionization time. In this fashion, a "spectrum" can be constructed using this composite model. To investigate whether the phase shift effect or the amplitude difference introduced have the largest influence, they can be individually inserted as modifications for the mock harmonic spectrum.

According to the calculations in the previous section, these modulations should be the same for all odd (and all even) harmonics. One may then simulate the intensity of an arbitrary harmonic, and introduce these one by one and in concert, to investigate their influence. An example of this can be seen in figure 11b on page 25.

To get the variables to use in equation (28), A and B are easily determined as the amplitude of the field at any given point, and the amplitude at another point π (one half cycle) removed. The phase Σ_3 can be calculated by using equation (24) on the preceding page for each of these points, and taking $\Sigma_3 = \Sigma_2 - \Sigma_1$.

[4]The "gate" is because, just like a logic gate, it can distinguish between conditions, in this case certain energies and trajectories.

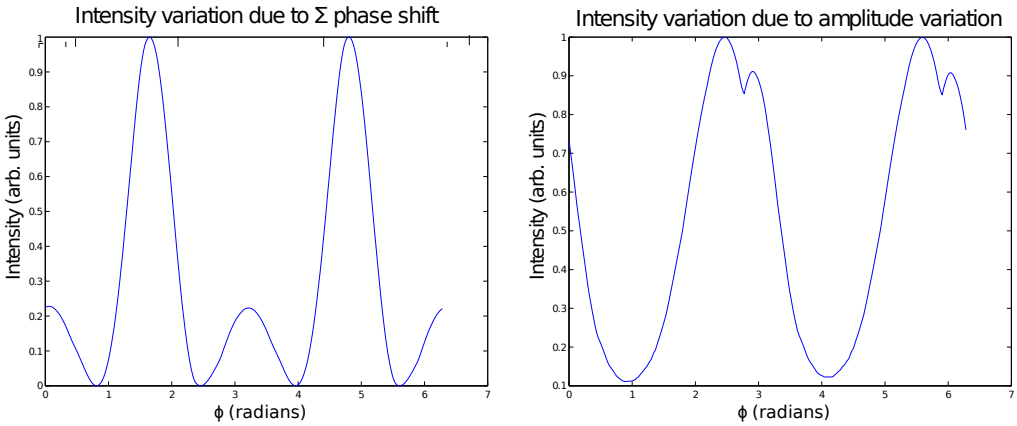

(a) Phase shift effect on spectrum. **(b)** Amplitude difference effect.

Figure 6: The intensity variation of the 23rd harmonic, arbitrarily chosen, but assumed to correspond with results for all odd harmonics.

2.7 Displacement gate

Recent papers [9, 10] give the assumption that when the 2ω field is perpendicularly polarized to the ω field, this will provide a *displacement gate*.

This is due to the fact that the "sideways" polarization will cause the electron to move away from the atom in a manner that it cannot simply recombine, since it's been displaced in the other direction. An illustration of this phenomenon can be seen in figure 7 on the next page.

Another assumption made in this model is that the perpendicularly polarized beam will not perturb the E-field and thus the ionization probability.

The electron has a certain probability of recombining, depending on its initial velocity. It must have a certain velocity in the y direction to offset the displacement given by the perpendicular field. The recombination probability, then, is at its largest when this "required" velocity $\dot{y}$ is as small as possible (because, on average, electrons' initial velocity in any given direction is zero).

Considering figure 7 on the following page, for this particular trajectory, the electron would have to have a velocity $\dot{y}'$ in the opposite direction of the transverse movement. The amount would have to be such that $\dot{y}' \cdot t$ is equal to the displacement.

A more mathematical way of putting this is that y and x should be zero

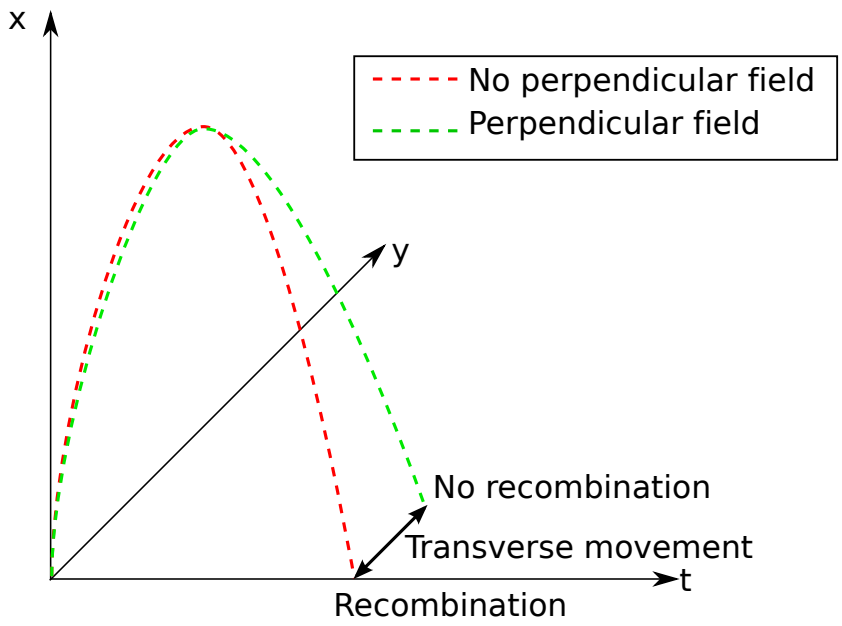

Figure 7: An illustration of the displacement gate introduced by a perpendicularly polarized second field. The red trajectory shows an electron moving back and forth in the x dimension as a function of time, after a while recombining with the atom at $x = 0$. The green trajectory does not, because the electron has moved away from the atom in the y dimension.

at the same time, and for this to be true, equation (16) on page 10 together with $\ddot{y}' \cdot (t_r - t_i)$ should be zero at $t = t_i$. The initial velocity $\ddot{y}'$ in this case means the velocity of the electron at the time of ionization.

Assuming a (somewhat arbitrary) velocity distribution Δv_{0y}, the displacement gate can be calculated as [10]

$$G(t_r, t_i, \phi) = \exp\left(-\frac{1}{2} v_{0_y}^2(t_r, t_i, \phi) \;/\; \Delta v_{0_y}^2\right). \tag{30}$$

Deriving $v_{0_y}(t_r)$ follows from

$$F_y(t) = m\ddot{y} = -eE_{2\omega}(t) \tag{31}$$

where

$$E_{2\omega}(t) = E_{0_{2\omega}} \cos(2\omega t + \phi) \tag{32}$$

and thus

$$\ddot{y}(t) = -\frac{eE_{0_{2\omega}}}{m} \cos(2\omega t + \phi) \tag{33}$$

The velocity can then be calculated by integrating the acceleration and adding v_{0_y}:

$$\dot{y}(t) = v_{0_y} + \int_{t_i}^{t} -\frac{eE_{0_{2\omega}}}{m}\cos(2\omega t' + \phi)\ dt' =$$
$$-\frac{eE_{0_{2\omega}}}{2m\omega}\left[\sin(2\omega t_i + \phi) - \sin(2\omega t + \phi)\right] + v_{0_y} \tag{34}$$

Given that for the electron to recombine with the atom, $y(t_r)$ must be 0:

$$\int_{t_i}^{t_r} \dot{y}(t)\ dt = 0$$
$$\Rightarrow \int_{t_i}^{t_r} \left(-\frac{eE_{0_{2\omega}}}{2m\omega}\left[\sin(2\omega t_i + \phi) - \sin(2\omega t + \phi)\right] + v_{0_y}\right) dt = 0 \tag{35}$$

which leads to

$$\int_{t_i}^{t_r} v_{0_y} dt = \int_{t_i}^{t_r} -\frac{eE_{0_{2\omega}}}{2m\omega}\left[\sin(2\omega t_i + \phi) - \sin(2\omega t + \phi)\right] dt \tag{36}$$

$$v_{0_y}(t_r - t_i) = -\frac{eE_{0_{2\omega}}}{2m\omega}\left[(t_r - t_i)\sin(2\omega t_i + \phi) + \frac{\cos(2\omega t_r + \phi) - \cos(2\omega t_i + \phi)}{2\omega}\right] \tag{37}$$

$$v_{0_y} = -\frac{eE_{0_{2\omega}}}{2m\omega}\left[\sin(2\omega t_i + \phi) + \frac{\cos(2\omega t_r + \phi) - \cos(2\omega t_i + \phi)}{2\omega(t_r - t_i)}\right]. \tag{38}$$

Inserting this into equation (30) on the preceding page gives

$$G(t_r, t_i, \phi) = \exp\left(-\frac{1}{2}v_{0_y}^2(t_r, t_i, \phi)\ /\ \Delta v_0^2\right)$$
$$= \exp\left(-\frac{e^2 E_{0_{2\omega}}^2}{m^2 8\omega^2 \Delta v_0^2}\left[\sin(2\omega t_i + \phi) + \frac{\cos(2\omega t_r + \phi) - \cos(2\omega t_i + \phi)}{2\omega(t_r - t_i)}\right]^2\right). \tag{39}$$

The second term can be dismissed because this function is much slower given a reasonably long return time [10]. This means that the ionization time can now be calculated from ϕ, the phase difference between the ω and 2ω fields, and vice versa. A simulation of the displacement gate as a function of ϕ and t_i can bee seen in figure 8 on the next page.

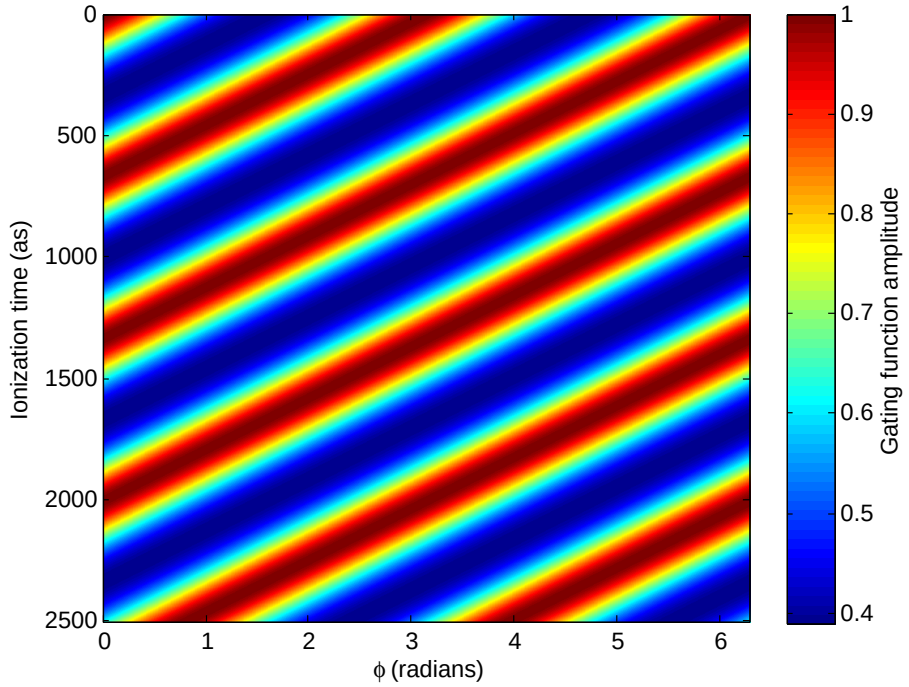

Figure 8: A plot of the displacement gate as a function of ionization time and phase shift, as given by equation (39) on the previous page.

2.8 A combination of approaches

Making a few assumptions, the displacement gate described in section 2.7 can be combined with the ionization gate described in section 2.6 to give a more complete picture of the ionization and recombination of electrons, considering an arbitrary polarization of the 2ω field.

The first assumption keeps the previously stated assumption that a perpendicularly polarized beam does not perturb the field, and extending it by asserting that the perpendicular component of an arbitrarily linearly polarized 2ω field will not perturb it either. Following in the same vein, it is assumed that the displacement gate will depend solely on the perpendicular component.

As the perpendicular component of the 2ω field does not perturb the

ionizing field, it is then assumed that the tunneling rate perturbation depends only on the parallell component.

As the two functions cause modulations of the harmonic intensity, a fundamental assumption of this report is that they can then be multiplied together.

2.9 Phase matching

Previous chapters have mainly been concerned with the *single atom response*, i.e. simply the interaction between one atom, by itself, and the EM field [5]. However, measuring the signal from a single atom is not possible due to the density of the sample. Instead, the interaction of a multitude of atoms with the field must be considered, and this gives rise to macroscopic effects.

The governing factor is the *wave vector mismatch* between the induced polarization and the generated harmonic. This consists of four terms: $\Delta\vec{k}_q$, the mismatch due to the intensity dependent dipole phase, $\Delta\vec{k}_g$, the geometrical mismatch, $\Delta\vec{k}_n$ and $\Delta\vec{k}_e$, mismatch due to dispersion by neutral atoms and free electrons, respectively.

At low gas pressures and long focal lengths, as in the later considered experiment, $\Delta\vec{k}_q$ is the dominant factor, and is the only one that differs for long and short trajectories[5]. It can be approximated (along the direction of propagation) as $\Delta\vec{k}_q = -\alpha\partial I/\partial z$, where α is a proportionality constant and I is the intensity.

In a focused beam, the intensity varies along the direction of propagation, and because of this, the phase matching of the two trajectories depends on α. It is large for the long trajectories, meaning their phase shifts swiftly along the direction of propagation (and generation), and that their light is more likely to be cancelled out at some point. Conversely, it is small for the short trajectories, giving in turn that they are less likely to be cancelled out and thus probably will end up with a higher intensity at the point of observation.

[5]See section 2.4 on page 8.

3 Equipment and Method

3.1 Experimental setup

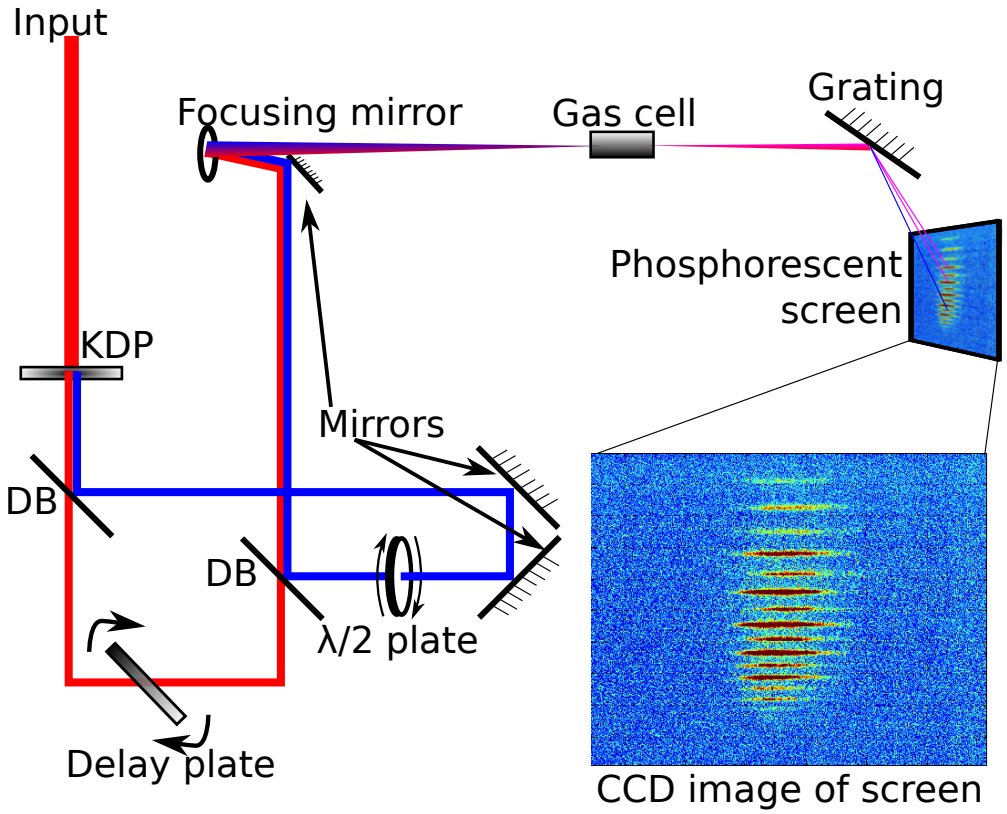

Figure 9: An illustration of the setup. The initial beam enters the KDP chrystal and generates the second harmonic. The red beam then travels through a dichroic beamsplitter (DB) and the delay plate. It is then reunited with the blue beam at another dichroic beamsplitter. Meanwhile, the blue beam has been led through a $\lambda/2$ plate to rotate its polarization. The two beams are then focused into the gas cell. The harmonics generated are then led via a grating onto a multi-channel plate, and a phosphorescent plate connected to a CCD.

The experiments were performed using a 10 Hz, 800 nm titanium sapphire laser. The second harmonic was generated by a KDP crystal. At the time of experiment measurements, the fundamental and second harmonic pulses were found to have pulse energies of 12 mJ and 0.38 mJ, respectively, thus the relative amplitude of the blue field was about 18%. This is just an estimate, however, which may be off mainly for two reasons. One is that two Gaussian beams with different wavelengths will have different beam sizes in the focal point. The other is that the gas cell may exhibit other nonlinear effects than just harmonic generation, among them Kerr lensing, which may lead to a beam being focused by the medium.

To separate the two beams, dichroic beamsplitters were used. These transmit a vast majority of the red beam and reflect most of the blue beam.

To control the delay ϕ, a glass disk was put on a motorized rotary stage in the beam line of the fundamental beam and rotated over 100 steps. This varies the amount of glass in the beam path, and thus its time of arrival.

To control the angle of polarization of the second harmonic, a motorized $\lambda/2$ plate was put in its beam line, its polarization rotated in 15 steps.

In total, this means that 1500 configurations were recorded in what's known as a 2D scan (because it scans over two variables). To compensate for random errors, 10 shots were taken for each configuration.

The laser was focused using a concave mirror with 2 m focal length, into a gas cell where it interacted with an argon gas jet.

An XUV grating spectrometer was then used to analyze the harmonics generated. This instrument has a grating, on which the light is incident. Light of all relevant wavelengths is then reflected onto a Multi-Channel Plate, which works as a 2D array of tiny photomultipliers. Because of a high potential difference between its two sides, light entering at any point on this 2D surface will cause an "avalanche" of electrons on the other side. The electrons then strike a phosphorescent plate, which is in turn captured by a simple digital camera (CCD).

3.2 Data processing

An overview of the collected data and the way it was processed can be seen in figure 10 on the next page. The data collected using the CCD camera was input into MATLAB. As 10 images were taken for each configuration (phase and polarization), all of these were averaged. Background radiation,

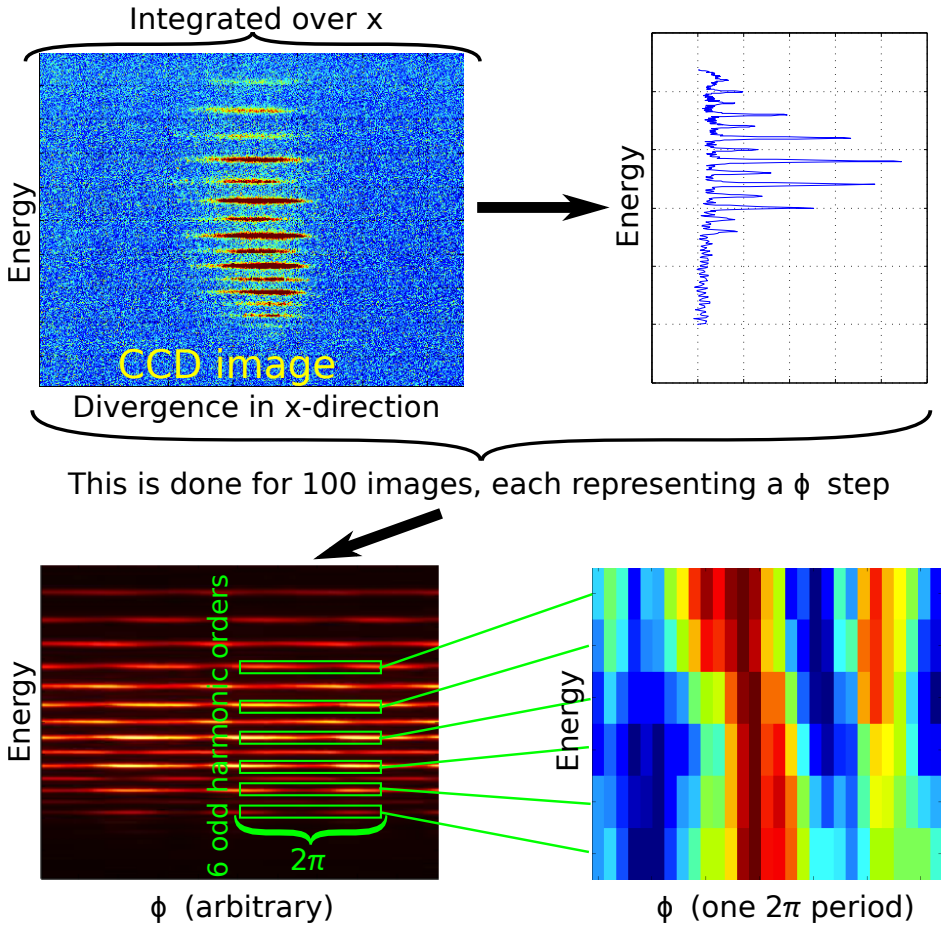

Figure 10: An illustration of the data processing. From left to right, top to bottom: the raw data from the camera, an integration over x for that particular image, 100 such integrations arranged side by side, and six "sifted out" harmonic spectra.

measured separately[6], was then subtracted from the data matrix.

After that, the data were summed over the x direction, which simply showed the angular divergence of the various harmonics. These data were not deemed relevant to the experiment, although some information can be acquired [4]. The result of the integration can be seen in the top right image. The data can now be seen as a column vector representing the energy span,

[6]Not shown in image, as it does not look particularly interesting.

with each element showing the intensity at that particular energy.

100 of these column vectors, one for each step of phase modulation, were then put together into a matrix, visualized as the bottom-left image. This, then shows the intensity of emissions as a function of energy (which harmonic order) (y direction) and phase (x direction).

Finally, the six most prominent odd harmonic orders were selected. The reason for using odd harmonics is that even harmonics require a parallel component of the 2ω field. This means they would not show up when one expects to study the displacement gate (see section 2.7 on page 16). A thin region around the main line of each harmonic order was summed in order to avoid numerical or measurement errors.

Using a cosine function, the periodicity of the intensity changes in the harmonics could be determined to the point where just a 2π wide "slice" could be selected from each. These six slices are shown in the bottom right image.

The maxima of each of these sifted-out harmonic spectra were then found using a small program to fit a Gaussian function onto their intensity curves.

3.3 Numerical methods

In order to establish parameters such as the electric field at t_i for each harmonic, at each relative phase and polarization, the equations for the propagation of the electron were evaluated numerically, giving a matrix of information similar to that plotted in figure 4 on page 12, which, for each possible ionization time, contained the return time and the return energy.

Since each harmonic has a fixed energy, it is then possible to scan through the energy matrix for its energy, to find the ionization times leading to that particular energy value. By knowing the expression for the field $E(t)$ at time t_i (see equation (6) on page 8), the ionization rate at t_i can be established.

At first, only the 'red' field was used in the calculations and an analytical expression was used for each of the relevant steps in section 2.4 on page 8. After several problems changing the expressions to fit a two-color field, the decision was made to switch to a numerical integration of each time step. This worked well but was exceedingly slow, so it was scrapped in favor of integrating the functions analytically using MATLAB's symbolic math functions.

4 Results

4.1 Simulation results

Phase and amplitude variation effects on harmonic spectrum

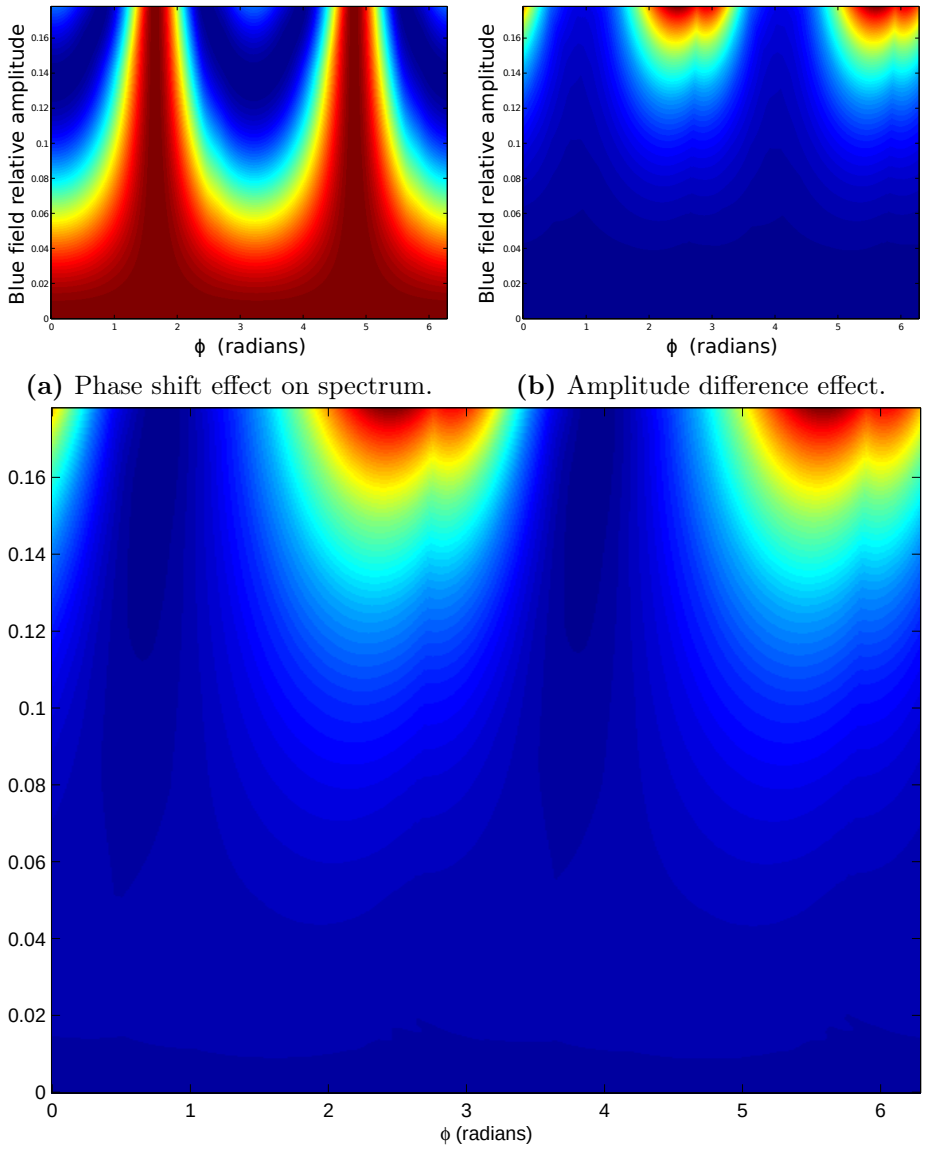

(a) Phase shift effect on spectrum.

(b) Amplitude difference effect.

(c) Total effect on spectrum.

Figure 11: A simulation of the intensity (colormap from blue to red) of the 23rd harmonic, varying with the phase and amplitude changes brought about by changes in ϕ shift and blue field intensity.

Using the models put together in section 2.6, the impact of the fluctuations in the fundamental field on the phase and amplitude of the harmonic fields, and their subsequent impact on the harmonic spectrum, could be studied, as in figure 11 on the preceding page. This picture shows the intensity of odd harmonics as a function of blue (2ω) field phase and intensity, normalized to the intensity at no blue field.

Figure 11a shows the intensity of the odd harmonics, considering just the phase shift (Σ_3 in equation (28)). Figure 11b shows the intensity when only the amplitude shift ($A \pm B$) is considered. In the first case, A and B are assumed to be equal, and in the second, Σ_3 is assumed to be zero.

Finally, figure 11c shows the intensity when both these factors are taken into account.

Figure 11a agrees particularly well with Fig 3b in [4]. As that article uses a very similar model for the phase, this is an indication that the implementation here works as intended.

What the image seems to show is that, in contrast with the assumption that the phase has a greater impact on harmonic intensity (and thus the harmonic spectrum), it seems that it is indeed the amplitude shift between the subcycles, enacted by the blue field phase shift, that proves the greater influence on the spectrum.

However, the maximum intensity of the 2ω field seems to affect this, as when the maximum intensity was increased, the importance of the amplitude shift increased even more. Thus, a reasonable prediction is that the phase may be the dominant factor if one has a very weak 2ω field.

This considers just the case of parallel polarization, because the perpendicular component of the 2ω field will not affect the ionization rate [10].

A combination of approaches, analyzed

A number of numerical simulations were carried out referring to section 2.8 on page 19, to study the effect on the harmonic spectrum of both the fluctuations in tunneling rate and the displacement gate.

Figure 12 on the following page shows a typical result, arbitrarily chosen, of the simulations, with the effect on the harmonic spectrum of the ionization gate on top, the displacement gate in the middle, and their product on the bottom. These simulations were performed on a variety of different blue field polarization directions, so as to give a reasonable approximation to the conditions of the experiment.

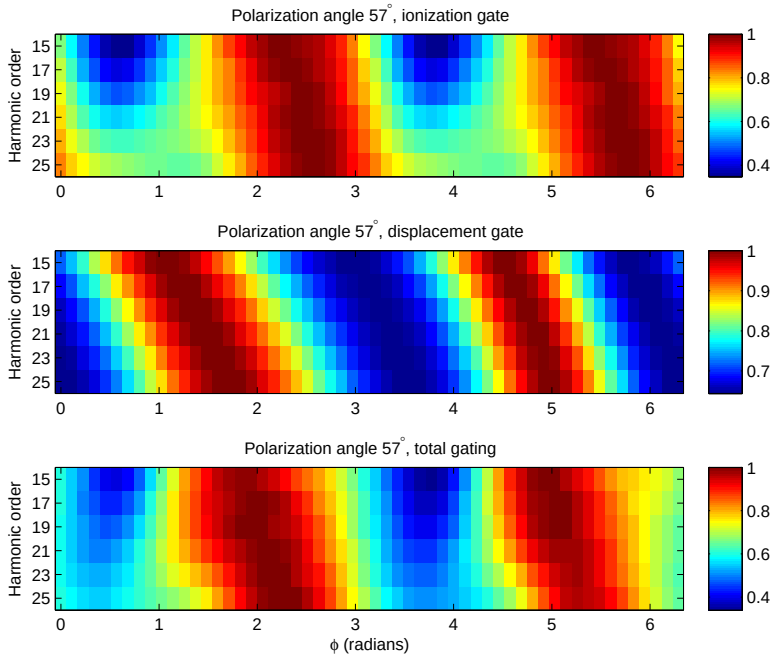

Figure 12: A simulation of the harmonic spectrum as a function of ϕ, considering the ionization gate (top), displacement gate (middle), and their product (bottom).

What the simulations show, in accordance with the theoretical assumptions, is that as the polarization varies, so does the importance of the two models; the ionization gate is essentially "flat" (1 everywhere) when the two fields are perpendicular (since, as the assumption of the gating model states, the perpendicular field does not perturb the ionization probability), and the displacement gate is likewise flat when the two beams are parallel (the displacement gate relies on the electron being moved perpendicularly to the ionizing field).

In the intermediate cases, one can see, as in the figure, that the "range" (how far from 1 the amplitude modulation goes) of a given model depends roughly on the cosine of the angle for the ionization gate and the sine of the angle for the displacement gate.

Interestingly, as can be seen in figure 12, outside of purely perpendicular conditions, the displacement gate is affected by the ionization gate perturbation caused by the blue field. This is obvious when one considers that the displacement gate depends not only on phase, but also on ionization time, which is changed by perturbations in the ionization gate.

4.2 Experimental results

Using the displacement gate to measure ionization time

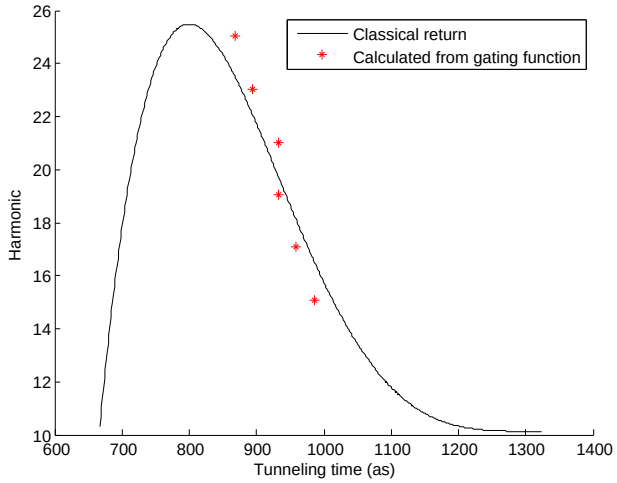

Figure 13: The classically calculated ionization times for different harmonic orders, along with measured data, whose ionization times have been calculated using the displacement gate method.

If the 2ω field is completely perpendicularly polarized, it is assumed [9] that it does not affect the actual ionization probability of the electron, i.e. it does not perturb the field in any way, as discussed in section 2.8 on page 19. A plot can be seen in figure 13, which shows both the classical calculation of the electron's energy from ionization time[7] and ionization times calculated using the displacement gate, with the phase ϕ deduced from experimental data. In this case, the phase values were extracted from what was determined to be the closest to perpendicular polarization.

The experimental setup makes it quite easy to determine the relative phase shifts between two given points, but there is no way of knowing the absolute phase. Therefore, the absolute phase was determined to be that

[7]The electron's propagation was calculated numerically using the equations in section 2.4 on page 8.

phase in which the calculated ionization times matched best with those given classically. This method holds credence as it is used by [10].

The fit is not perfect, nor is it expected to be, as there are some differences between the classical return function and the fully quantum mechanical treatment given to HHG, for example, in [6]. However, it agrees well enough that the assumption that the perpendicularly polarized component does not perturb the field seems to hold.

It is quite possible that none of the polarization steps, in which the experiment was performed, corresponds to a perfectly perpendicular polarization, and thus some perturbation will probably have been introduced by the parallel component.

Another possible source of errors or inaccuracies is the assumed intensities, both the field intensity in general and the relative intensities of the ω and 2ω fields. The fundamental field intensity determines the maximum harmonic order that can be reached[8]. The relative field intensity has a definite impact on the relative strength of the odd harmonics measured here[9].

Polarization and phase dependency of the harmonic spectrum

15 images were analyzed (one for each polarization step, as discussed in section 3.1 on page 21), and six odd harmonics were isolated from each frame, 15, 17, 19, 21, 23 and 25. On most frames, a "slope" can be seen across the image, following the maximum intensities of each harmonic, with the phase dependency clearly changing between them.

When viewed in succession, it is clear that the slope performs some kind of pendulous motion, apparently periodic with the polarization direction.

Comparing simulations to experimental data

The images of solely the harmonics discussed in the previous section were put together with the images produced as "a combination of approaches" for comparison. Figure 14 on the next page is presumably where the blue field is the closest to perpendicularly polarized, and this is also where the simulations agree the most with the experimental data.

As the perpendicularly polarized condition is in the displacement gate regime, a reasonable explanation for this is that close to completely perpen-

[8] See equations 17 and 18 on page 11.

[9] See section 2.5 on page 12.

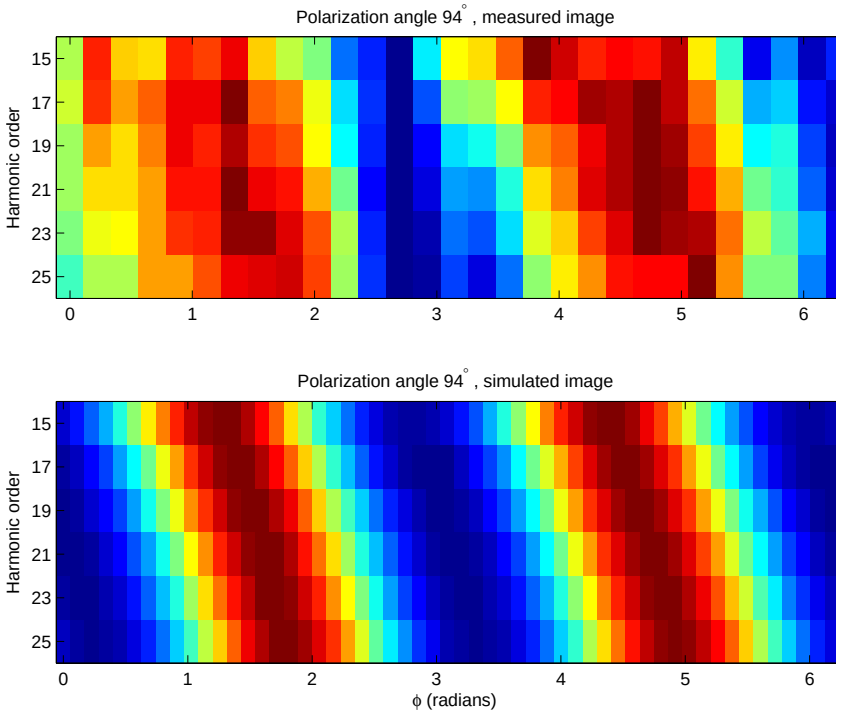

Figure 14: The measured data compared to the simulated at 94° polarization, probably the closest to perpendicular polarization, showing a very good correlation between simulation and reality.

dicular blue field conditions, the displacement gate is a very good model for the electrons' behavior.

The earlier, and later, polarization steps show a form of systemic error in the simulations, in which the higher orders involved (21-25) show the same kind of slope change (albeit much weaker) as in the experimental images but the lower orders do not. This could have a number of explanations, chiefly that the ionization gate model (or its implementation here) is still somewhat lacking, or the experimental conditions (laser intensity, focus, even energy) were not reproduced correctly in the simulations. Two examples of this are figure 15 and figure 16 on the following page.

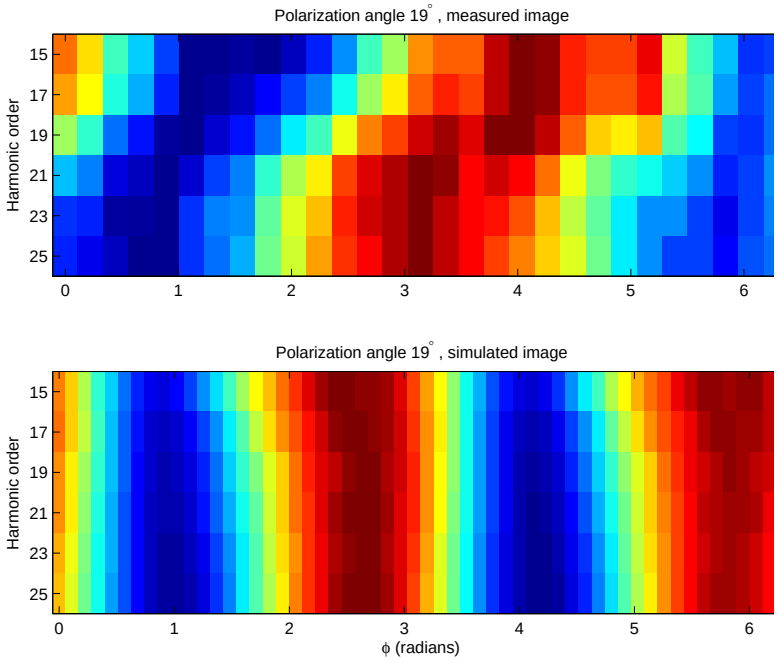

Figure 15: The measured data compared to the simulated at 19° polarization, showing a significant difference between simulation and reality.

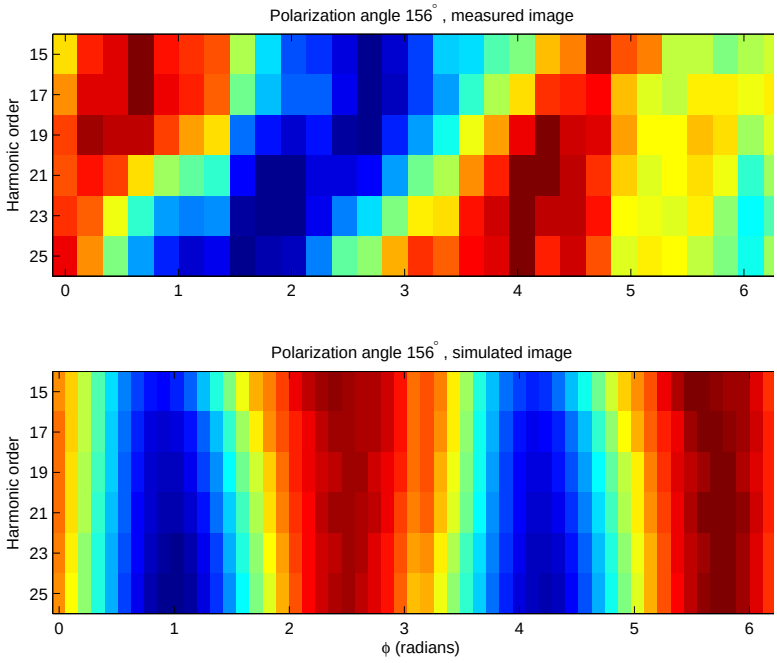

Figure 16: The measured data compared to the simulated at 156° polarization, with the simulation deviating from the measured image.

5 Outlook

There's certainly much to be done, both with the models and with the experimental data. Due to time constraints, only approximately half of the data from this experiment have so far been analyzed, and more data could well improve the results further.

Many approximations have been made, and it is possible that some may prove inaccurate or outright erroneous. However, many of the models, such as the displacement gating model and parts of the ionization gate, agree very well with experimental data and thus seem likely to hold some truth.

This thesis proved challenging from both a theoretical and technical point of view. Higher harmonic generation is a very current and evolving field of study, and it was very interesting to get some grasp of the theories and models put forth to explain it. Technically, it gave a good opportunity to become more aquainted with MATLAB as a scientific tool, and an insight into data handling in scientific experiments.

6 Acknowledgements

The author would like to thank Christoph Heyl first of all, for excellent support as a supervisor. Thanks are also due others at the Atomic Physics division: Anne l'Huillier, for making this thesis possible and for theoretical considerations, Piotr Rudawski for input on calibration of data, and Fernando Brizuela for information on the lab setup.

References

[1] M. Ammosov, N. Delone, and V. Krainov. Tunnel ionization of complex atoms and of atomic ions in an alternating electromagnetic field. *Journal of Experimental and Theoretical Physics*, 64(6):1191, 1986.

[2] E. Clementi, D. L. Raimondi, and W. P. Reinhardt. Atomic Screening Constants from SCF Functions. II. Atoms with 37 to 86 Electrons. *Journal of Chemical Physics*, 47:1300–1307, 1967.

[3] M. B. Gaarde, M. Murakami, and R. Kienberger. Spatial separation of large dynamical blueshift and harmonic generation. *Phys. Rev. A*, 74:053401, 2006.

[4] X. He, J. M. Dahlström, R. Rakowski, C. M. Heyl, A. Persson, J. Mauritsson, and A. L'Huillier. Interference effects in two-color high-order harmonic generation. *Phys. Rev. A*, 82:033410, 2010.

[5] C. M. Heyl, J. Güdde, A. l'Huillier, and U. Höfer. High-order harmonic generation with μj laser pulses at high repetition rates. *Journal of Physics B: Atomic, Molecular and Optical Physics*, 45(7):074020, 2012.

[6] M. Lewenstein, P. Balcou, M. Y. Ivanov, A. l'Huillier, and P. B. Corkum. Theory of high-harmonic generation by low-frequency laser fields. *Phys. Rev. A*, 49(3):2117, 1994.

[7] F. Lindner, W. Stremme, M. G. Schätzel, F. Grasbon, G. G. Paulus, H. Walther, R. Hartmann, and L. Strüder. High-order harmonic generation at a repetition rate of 100 khz. *Phys. Rev. A*, 68:013814, 2003.

[8] B. Saleh and M. Teich. *Fundamentals of Photonics, 2nd edition.* Wiley Series in Pure and Applied Optics. Wiley, 2007.

[9] D. Shafir, H. Soifer, B. D. Bruner, M. Dagan, Y. Mairesse, S. Patchkovskii, M. Y. Ivanov, O. Smirnova, and N. Dudovich. Resolving the time when an electron exits a tunnelling barrier. *Nature*, 485(7398):343–346, 2012.

[10] H. Soifer, M. Dagan, D. Shafir, B. D. Bruner, M. Y. Ivanov, V. Serbinenko, I. Barth, O. Smirnova, and N. Dudovich. Spatio-spectral analysis of ionization times in high-harmonic generation. *Chemical Physics*, 414(0):176 – 183, 2013.